

**CONNECTED
VEHICLE/INFRASTRUCTURE
UNIVERSITY TRANSPORTATION
CENTER (CVI-UTC)**

**CONNECTED VEHICLE FREEWAY SPEED
HARMONIZATION SYSTEMS**

Connected Vehicle Freeway Speed Harmonization Systems

Prepared for the Research and Innovative Technology Administration (RITA);
U.S. Department of Transportation (US DOT)

Grant Project Title:

Advanced Operations Focused on Connected Vehicles/Infrastructure (CVI-UTC)

Consortium Members:

**Virginia Tech Transportation Institute (VTI),
University of Virginia (UVA) Center for Transportation Studies,
and Morgan State University (MSU).**

Submitted by:

**Virginia Tech Transportation Institute
3500 Transportation Research Plaza
Blacksburg, VA 24061**

Program Director:

Dr. Thomas Dingus

Program Director, Connected Vehicle/Infrastructure
University Transportation Center
Director, Virginia Tech Transportation Institute
Professor, Department of Biomedical Engineering and Mechanics
at Virginia Tech
tdingus@vti.vt.edu
(540) 231-1501

Name of Submitting Official:

Hesham Rakha, Ph.D., P.Eng.

Director, Center for Sustainable Mobility, Virginia Tech
Transportation Institute
Samuel Reynolds Pritchard Professor of Engineering, Charles E.
Via, Jr. Dept. of Civil and Environmental Engineering, Virginia
Tech
hrakha@vt.edu
(540) 231-1505

Hao Yang, Ph.D.

Post-Doctoral Associate
Virginia Tech Transportation Institute

DUNS: 0031370150000

EIN: 54-6001805

Grant Funding Period: January 2012 – July 2016
Final Research Reports

March 15, 2016

Disclaimer

The contents of this report reflect the views of the authors, who are responsible for the facts and the accuracy of the information presented herein. This document is disseminated under the sponsorship of the U.S. Department of Transportation's University Transportation Centers Program, in the interest of information exchange. The U.S. Government assumes no liability for the contents or use thereof.

Connected Vehicle/Infrastructure UTC

The mission statement of the Connected Vehicle/Infrastructure University Transportation Center (CVI-UTC) is to conduct research that will advance surface transportation through the application of innovative research and using connected-vehicle and infrastructure technologies to improve safety, state of good repair, economic competitiveness, livable communities, and environmental sustainability.

The goals of the Connected Vehicle/Infrastructure University Transportation Center (CVI-UTC) are:

- Increased understanding and awareness of transportation issues
- Improved body of knowledge
- Improved processes, techniques and skills in addressing transportation issues
- Enlarged pool of trained transportation professionals
- Greater adoption of new technology

Abstract

The capacity drop phenomenon, which reduces the maximum bottleneck discharge rate following the onset of congestion, is a critical restriction in transportation networks that causes additional traffic congestion. Consequently, preventing or reducing the occurrence of the capacity drop not only mitigates traffic congestion, but can also produce environmental and traffic safety benefits. To address this issue, this project developed and evaluated a speed harmonization (SH) algorithm based on a bi-level feedback control system with the assistance of vehicle-to-infrastructure (V2I) communications. The algorithm computes advisory speed limits for individual vehicles to prevent the breakdown of downstream bottleneck discharge by regulating traffic flow approaching the bottleneck, which in turn reduces traffic stream delay, emissions and fuel consumption levels. To assess the benefits of the algorithm, a section of Interstate 66 in Northern Virginia was simulated with the INTEGRATION microscopic traffic simulation model, and five trailers were installed on the road to collect real-time traffic data for each vehicle equipped with V2I communications to implement the SH algorithm. The simulations demonstrated that the algorithm significantly mitigated road congestion when a capacity drop occurred at a bottleneck. Also, the study results showed that higher market penetration rates (MPRs) of vehicles equipped with the SH algorithm led to higher SH algorithm benefits. In particular, at 100% MPR, the bottleneck discharge flow rate increased by up to 1.5%, and the vehicular delay decreased by about 22%. Moreover, with the SH algorithm, CO₂ and fuel consumption levels were reduced by up to 3.5%. A 100% MPR is the best-case scenario. However, the results also demonstrated that an MPR of even 10% is sufficient to produce overall emission and fuel consumption savings.

Acknowledgements

The authors recognize the support that was provided by a grant from the U.S. Department of Transportation – Research and Innovative Technology Administration, University Transportation Centers Program and to the Virginia Tech Transportation Institute.

Table of Contents

Background.....	5
Introduction.....	5
Relevant Work.....	5
Project Tasks.....	7
Method.....	7
Capacity Drop at Bottlenecks.....	8
Speed Harmonization Algorithm.....	9
Results and Discussion.....	15
Base Case Analysis.....	15
Case study I: SH Algorithm and Three V2I-Equipped Vehicles.....	17
Case Study II: SH Algorithm and 100% V2I-Equipped Vehicles.....	19
Case Study III: Different Market Penetration Rates.....	20
Conclusions.....	23
References.....	24

List of Figures

Figure 1. Diagram of a lane-drop bottleneck.	8
Figure 2. Fundamental diagram at a simple lane-drop bottlenecks.	9
Figure 3. Lane-drop bottleneck with on- and off-ramps.	10
Figure 4. SH algorithm feedback control schematic.	13
Figure 5. Flow chart of the SH algorithm.	14
Figure 6. Diagram of I-66 network.	15
Figure 7. Speed profiles along I-66.	16
Figure 8. Flow rate at the bottleneck.	17
Figure 9. Comparison of speed profiles on I-66 with three vehicles.	19
Figure 10. Comparison of speed profiles along I-66 with 100% equipped vehicles.	20
Figure 11. Impact of MPRs on the SH algorithm: (a) delay and flow rate at the bottleneck, (b) emissions and fuel consumption.	22

List of Tables

Table 1. Settings of the SH Algorithm.	18
Table 2. Simulation Results with Three Equipped Vehicles	19
Table 3. Simulation Results with 100% Equipped Vehicles	20

Background

Introduction

The rapid growth of urban vehicular traffic has resulted in serious traffic congestion. Congestion causes various problems in transportation systems, such as capacity drop at bottlenecks, increased risk of traffic incidents, and high emissions and fuel consumption. Studies by Parry [1] showed that in the U.S., one third of greenhouse gas emissions were caused by the transportation sector, and 80% involved passenger cars and freight trucks. Globally, the situation has also worsened due to the rapidly increasing numbers of motor vehicles in developing countries [2]. Moreover, traffic congestion caused about 5 billion hours of delay for commuters and cost over 100 billion dollars per year over the past 10 years [3].

The capacity drop at a bottleneck, which occurs after the onset of congestion and reduces the bottleneck discharge rate, is one critical cause of traffic flow instability and one significant restriction in network performance. This concept of capacity drop was first analyzed by Edie [4], who showed that the discharge flow rate of the Lincoln Tunnel, which connects New Jersey and New York, was reduced when the vehicle density in the tunnel was higher than 70 vehicles per mile. Bank investigated the capacity of a freeway merging section with an on-ramp and found that the capacity decreased about 3–10% once queues formed upstream [5]. Hall and Angyemang analyzed traffic flow data from the Queen Elizabeth Way (QEW), Toronto, Canada, and concluded that the bottleneck capacity was reduced by approximately 6% when a queue formed at the bottleneck [6]. In addition, several on-ramp bottlenecks were studied to analyze capacity drop [7, 8]. Persaud et al. studied the relationship between capacity drop at the on-ramp merge area and the upstream demand [9], and found that the probability of capacity drop was a function of the demand, and that the capacity was reduced 10–16% when the upstream of the bottleneck was congested. Furthermore, Chung et al. studied the relationship between the capacity drop and traffic density and found that capacities at bottlenecks on Interstate 85 in San Diego, CA were reduced by 8–18% when the traffic density at the upstream of the bottleneck was larger than 24 vehicles per km per lane [9]. Chamberlayne et al. applied INTEGRATION software [10, 11] to model capacity drop under various bottleneck configurations and showed that the capacity was reduced by about 5–20% under different demand levels [12]. This study also demonstrated the capability of the INTEGRATION software in replicating capacity drop at freeway bottlenecks.

Relevant Work

Much work has been done to improve the discharge flow rate at bottlenecks. Given the mechanism of capacity drop as it is explored in the literature, the most intuitive way of addressing this problem is mitigating traffic congestion or releasing queues at the upstream of bottlenecks.

In the literature, three methods are proposed to prevent capacity drop from occurring at bottlenecks. The first method is ramp-metering, which controls entering flow rates of on-ramps. For example, Papageorgiou et al. developed ALINEA local ramp metering, which utilized an integral controller to regulate metering rate and to adjust the downstream flow rate to be within the road capacity [13, 14]. The method was capable of reducing overall travel time by about 8% during peak hours on an urban corridor in Paris [15]. In several other studies [16-18], ramp metering was also demonstrated to mitigate queues in the shoulder lane as well as to achieve higher discharge flow rates of diverging or merging bottlenecks. Chung et al. adjusted the metering rate of an on-ramp by monitoring the density at the upstream of the bottleneck [19]. The results indicated that a traffic-responsive scheme to control density held promise, as it increased bottleneck discharge flow rates. However, ramp metering requires that an on-ramp exist upstream of the bottleneck, and consequently, is not appropriate for lane-drop bottlenecks, or bottlenecks caused by work zones. Furthermore, on-ramp storage space is typically limited, thereby limiting the control that can be carried out there. The second method of mitigating capacity drop is installing mainstream traffic signals [20, 21] toll plazas [22, 23], which also efficiently regulate mainstream traffic flows arriving at bottlenecks in an attempt to maximize the bottleneck throughput. Papageorgiou et al. used a feedback control system based on the ALINEA algorithm [13] to prevent road congestion from building up, thus increasing the bottleneck throughput. However, this application has limited practicality due to the high installation and maintenance costs of the required infrastructures along with an inability to deal with non-recurrent bottlenecks. Furthermore, this type of control still forces vehicles to come to a complete stop and thus would have limited energy and environmental benefits.

With the help of the connected vehicle technologies, both vehicles and roadside units are able to collect real-time disaggregate and aggregate road traffic conditions. Hence, Variable Speed Limits (VSLs), which provide dynamic speed limits to drivers through either on-board message signs or in-car devices, have the potential to achieve the desired outcome with minimum infrastructure costs. VSLs control flow rates on the freeway by restricting vehicle speed limits, which in essence meters traffic on the mainline. This approach is very attractive because it does not force traffic to come to a complete stop and thus has the potential of producing significant energy and environmental benefits in addition to the desired increase in throughput benefits. With this in mind, Hegyi et al. implemented VSL to reduce the travel time of vehicular trips and eliminate traffic oscillations along a roadway segment [24, 25]. However, they did not consider its benefits on traffic mobility. In the last decade, mainstream traffic flow control, a novel VSL control system operated either by optimal control [26] or local feedback control [27-30], has attracted researchers as a way to mitigate capacity drop at bottlenecks and traffic blocking at off-ramps. However, systems proposed are typically reactive rather than proactive. Specifically, these reactive systems monitor the occupancy upstream of the bottleneck and attempt to maintain it at a specific, uncongested level. For example, Jin and Jin analyzed the effect of VSL on mitigating the capacity drop at a lane-drop bottleneck [31]. In their study, a VSL algorithm based on a proportional-integral (PI) controller was proposed to maintain traffic conditions at the bottleneck at the desired

steady states without a capacity drop, with the result being a significant increase in bottleneck discharge rate. Chen et al. developed a VSL control system on freeways for fixed and non-recurrent freeway bottlenecks [32, 33]. The VSL algorithm controlled upstream traffic to dissipate the queue upstream of a bottleneck, and then regulated the inflow to the bottleneck to maintain a stable maximum discharge rate without breakdown. However, the drawbacks of both Jin and Jin's and Chen's studies are two-fold. First, the development of the algorithms is based on the analysis of steady-state traffic. However, in reality, there exist transient states and stochastic variability in traffic conditions that reduce the effectiveness of the algorithm. Second, the benefits of the algorithm were only quantified using a kinematic wave model, where the influence of lane differences and lane changes is not accounted for, even though studies by Munoz et al. and Laval et al. [18, 34] showed that these two factors were major causes of capacity drop at bottlenecks. The advantages of the algorithms are then over-estimated given the deterministic nature of the simulations.

Project Tasks

To address the influence of capacity drop and overcome the drawbacks of existing studies, this project proposed a speed harmonization (SH) algorithm based on a bi-level feedback control system to proactively prevent capacity drop [35]. The algorithm computed advisory speed limits for one network link based on traffic information collected by detectors located upstream of a bottleneck to (1) restrict the traffic flow to dissipate any existing congestion directly upstream of the bottleneck, and (2) maintain the maximum bottleneck discharge rate. In addition, to prevent the risk of incidents and low compliance rates caused by abrupt decelerations in the SH zone, vehicle-to-infrastructure (V2I) communications were introduced to provide the speed limit for each individual V2I-equipped vehicle. Moreover, to evaluate the advancement of the algorithm, the project applied a microscopic traffic simulation model, INTEGRATION [10, 11] which was able to simulate the driving behaviors of each vehicle and calculate corresponding emissions and fuel consumption through the VT-Micro Emission Model [36]. A freeway segment on Interstate 66 in Northern Virginia was simulated to assess the algorithm's benefits on improving the discharge flow rate of the bottleneck, reducing the delay of the vehicular trip, and decreasing emissions and fuel consumption. Furthermore, we analyzed the impact of market penetration rates (MPR) of equipped vehicles on the effectiveness of the proposed algorithm.

Method

Bottlenecks are a major cause of traffic congestion in transportation networks. Empirical studies have shown that the breakdown of bottlenecks results in a further reduction in the bottleneck discharge flow rate, which is typically referred to in the literature as the capacity drop. This capacity drop results in even more congestion on the roadways. In this report, we propose an SH algorithm to gate the traffic reaching the downstream bottleneck, thus ensuring that the bottleneck does not break down.

Capacity Drop at Bottlenecks

Generally, capacity drop occurs at road bottlenecks, such as the number of lanes is reduced. Figure 1 illustrates a simple lane-drop bottleneck, where the number of lanes of a freeway segment changes from two to one. As stated in Chung et al. [19], once a queue forms at the upstream of the bottleneck, (i.e., the upstream of the bottleneck is congested), the maximum discharge flow rate will be reduced.

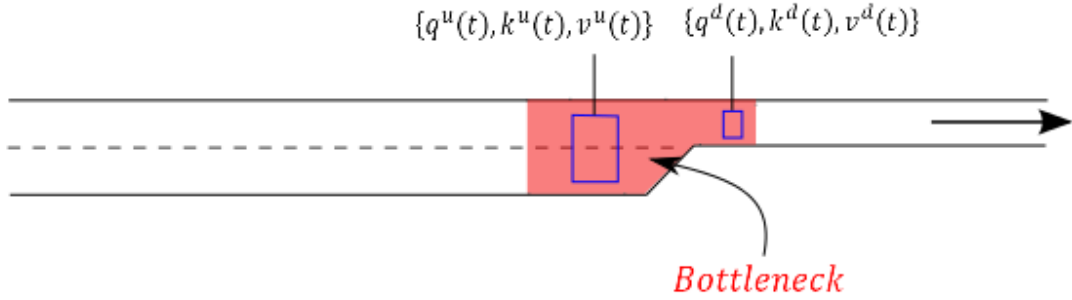


Figure 1. Diagram of a lane-drop bottleneck.

In Figure 1, two detectors are installed on the mainline freeway, and $\{q_u(t), \rho_u(t), v_u(t)\}$ and $\{q_d(t), \rho_d(t), v_d(t)\}$ represent the flow rate, density, and speed from the detectors at the upstream and downstream of the bottleneck, respectively. Figure 2 shows the fundamental diagram at the bottleneck. The solid black lines represent the flow-density relationships at the upstream and downstream of the bottleneck without capacity drop. Here, $\{q_{u,c}, \rho_{u,c}, \rho_{u,j}\}$ and $\{q_{d,c}, \rho_{d,c}, \rho_{d,j}\}$ signify the capacity, density at capacity, and jam density at the upstream and downstream of the bottleneck, respectively, and we let $q_{d,c} \leq q_{u,c}$. The bottleneck capacity is determined by the downstream road capacity of the bottleneck; $q_{d,c}$. Once a queue forms at the upstream of the bottleneck (i.e., the upstream of the bottleneck is congested) ($\rho_u(t) > \rho_{u,c}$), the maximum discharge flow rate of the bottleneck decreases to $(1 - \delta)q_{d,c}$, where δ is the percentage of capacity drop. The fundamental diagram at the upstream of the bottleneck with capacity drop is illustrated by the blue solid line in Figure 2.

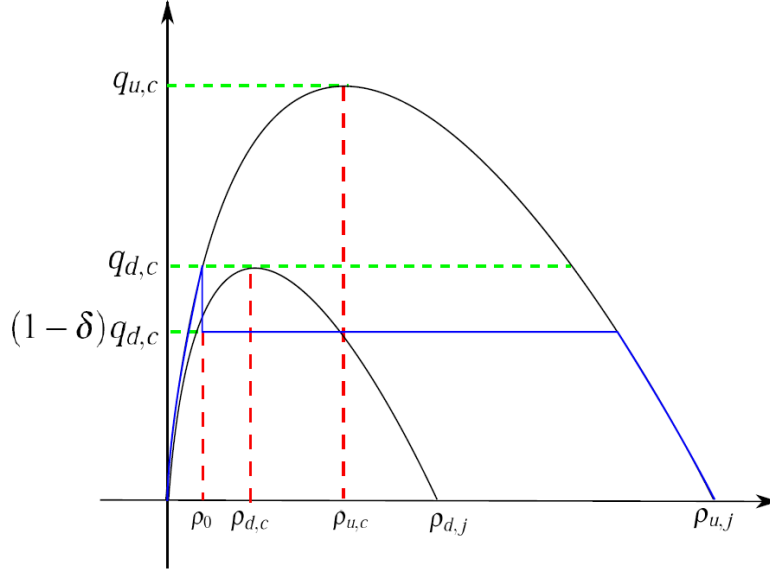


Figure 2. Fundamental diagram at a simple lane-drop bottlenecks.

When the demand at the origin of the road, d , is less than $(1 - \delta)q_{d,c}$, capacity drop does not occur on the road; if $d > (1 - \delta)q_{d,c}$, capacity drop at the bottleneck always exists. The rest of the scenario with $(1 - \delta)q_{d,c} < d < q_{d,c}$ is a little more complicated. In this scenario, capacity drop occurs only when the upstream of the bottleneck is initially congested; otherwise, the capacity of the bottleneck is still $q_{d,c}$.

Speed Harmonization Algorithm

Figure 2 indicates that there is an optimal density that can maximize the discharge flow rate of the bottleneck as well as eliminate the capacity drop (we define this density as the target density). In this project, we developed a speed harmonization algorithm with the assistance of V2I communications. The SH algorithm provides advisory speed limits to individual vehicles to control the upstream influx of a bottleneck to ensure the upstream density does not exceed a target density and to maximize the out-flux of the bottleneck. In this algorithm, speed limits are estimated not only based on the road traffic conditions, but also from the speed when the vehicles are entering the control zone. In this way, each driver can receive a comfortable suggestion about the advisory speed limit, and at the same time the algorithm can obtain environmental benefits on the whole road segment.

The SH algorithm is shown below in Figure 3, which illustrates a lane-drop bottleneck on a freeway. The road section is divided into three zones: a) the speed harmonization (SH) zone, b) the acceleration zone, and c) the bottleneck. In order to develop an SH algorithm, we placed three sets of detectors that gathered traffic volume, speed and occupancy data for use in the algorithm: one in the SH zone, one directly upstream of the bottleneck, and one directly downstream of the bottleneck. If on- and/or off-ramps exist between the SH zone and the bottleneck, detectors are needed at the on- and off-ramps to record the traffic flow. V2I-equipped vehicles in the SH zone

received advisory speed limits from the traffic management center (TMC) to control the flow arriving at the bottleneck.

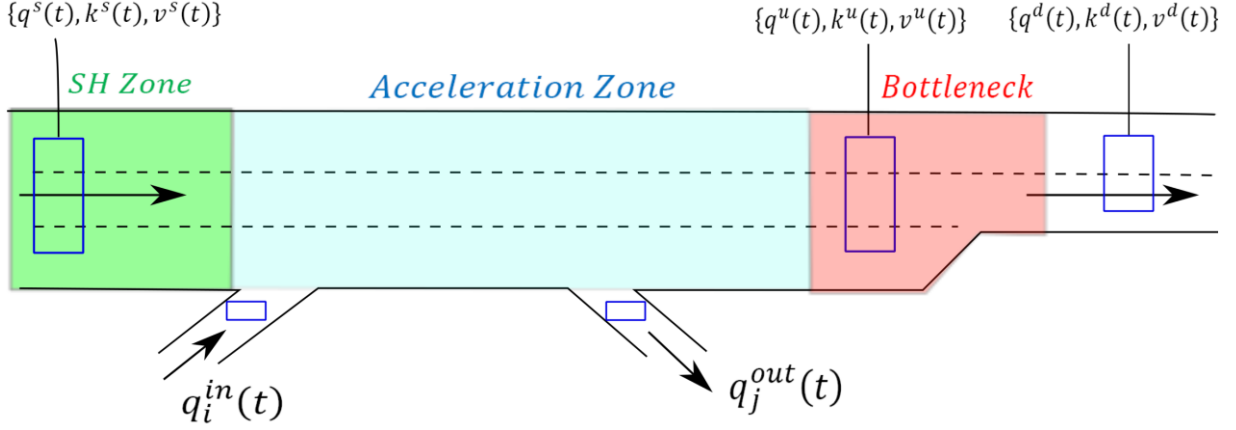


Figure 3. Lane-drop bottleneck with on- and off-ramps.

From Figure 2, we made the assumption that the flow-density and speed-density relationships were $q = Q(k), v = V(k)$. In order to prevent traffic breakdown upstream of the bottleneck, we constrained the arrivals at the bottleneck. Here, we set a target density, ρ_0 (or its equivalent occupancy given that density cannot be measured in the field), in order to achieve the desired objective. We controlled the in-flow rate of the bottleneck at q_c^d (i.e., the capacity of the bottleneck). The primary objective function of the speed harmonization algorithm was to maximize a weighted combination of the flow downstream of the bottleneck and speed variability within the speed harmonization section as:

$$\max_{v_0(t)} \sum_{t=1}^T w_q q^d(t) + \frac{w_v}{\tilde{v}^s(t)}$$

s.t.

$$\begin{aligned} k^u(t) &\leq k_c^u; \\ \hat{q}^s(t) &\leq q_c^d + q_r(t); \\ \Delta v(t) &\leq \Delta v_{thr}; \\ \tilde{v}_0(t) &\geq v_{min}. \end{aligned}$$

Where:

$\tilde{v}_0(t)$: the advisory speed limit in the SH zone at instant t ;

w_q : the weight assigned to the flow directly downstream of the bottleneck;

w_v : the weight assigned to the speed variability in the SH zone;

\tilde{v}^s : a measure of the speed variability in the SH zone;

$q_r(t)$: the sum of flow rates at all on- and off-ramps between the SH zone and the bottleneck at instant t ;

$\hat{q}^s(t)$: the flow rate at time t in the SH zone;

k_c^u : the desired density directly upstream of the bottleneck;

$\Delta v(t)$: the difference between the speed advisory speed limits over the control interval in the SH zone at time t ;

T : the total simulation time;

Δv_{thr} : the maximum allowed change in the control speed in the SH zone;

v_{min} : the minimum advisory speed limit;

$q^d(t)$: the discharge flow rate of the bottleneck at instant t , and it is restricted by $\hat{q}^s(t)$.

The objective function was to maximize the bottleneck throughput and minimize the speed variability within the SH zone. The addition of the second term would require some probe vehicles in the SH zone to monitor the speed variability.

Here, $\rho_c^u = \rho_0$ is one criterion to determine when the SH should be activated. Also, we estimated $q_r(t)$ using the following function,

$$q_r(t) = \sum_j q_j^{out}(t + l_j^{out}) - \sum_i q_i^{in}(t + l_i^{in}).$$

Here, l_j^{out} is the lag for vehicles traveling from the SH zone to the off-ramp j , and l_i^{in} is the lag from the SH zone to the on-ramp i . The lags were computed assuming that vehicles traveled from the SH zone to the given locations at the free-flow speed or potentially at the prevailing traffic stream space-mean speed. In that sense, some method was needed to predict these flows, and further investigation into the optimum smoothing/prediction algorithm was undertaken.

The advisory speed limit, $\tilde{v}_0(t)$, was estimated to achieve the optimal flow rate in the SH zone, $\tilde{q}_0(t)$. We defined two reverse functions of the flow-density and speed-density relationships under congested traffic for the upstream of the bottleneck.

$$\begin{aligned} \rho &= V^{-1}(v) & \rho_c^u \leq \rho < \rho_j^u; \\ \rho &= Q^{-1}(q), & \rho_c^u \leq \rho < \rho_j^u. \end{aligned}$$

A feedback Bang-Bang dual control system (see Figure 4) is introduced to realize the algorithm and solve the optimization problem. The feedback system ensures the robustness and stability of the algorithm, and the moving average component in the system enables the algorithm to work with transient states when the capacity drop occurs. **Error! Reference source not found.** illustrates the flow chart of the algorithm. The algorithm is described below.

1. When $t \leq t_0$, we assign the advisory speed limit in the SH zone as

$$\tilde{v}_0(t) = v_f,$$

The optimal flow rate at the SH zone is set as

$$\tilde{q}_0(t) = q_c^d + q_r(t).$$

Here, t_0 is the starting time when the algorithm is activated.

2. At each time step t , we check the following two conditions:

$$\begin{cases} q^s(t) < q_c^d + q_r(t) \\ \rho^u(t+l) \leq \rho_c^u \end{cases}.$$

Here, l is the time lag for vehicles traveling from the SH zone to the bottleneck. $l = L/v_l$, where L is the distance from the SH zone to the bottleneck, and v_l is either the free flow speed or the space-mean speed of the prevailing traffic stream.

- a. If both conditions are satisfied, we set the advisory speed limit as

$$\tilde{v}_0(t+1) = v_f.$$

- b. If either one of the conditions is violated, we first compute the target flow rate in the SH zone.

$$\hat{q}_0(t+1) = \beta \cdot q_c^d + q_r(t),$$

where, β is the coefficient for the bottleneck capacity. If $\rho^u(t+l) > \rho_c^u$ and $|\tilde{v}(t) - \tilde{v}(t-1)| < \Delta v_{thr}$, we set $\beta = \beta_0$, where β_0 is the coefficient of the bottleneck capacity, and $\beta_0 < 1$. Then, $\beta \cdot q_c^d$ is less than the maximum discharging flow rate of the bottleneck when capacity drop happens. Otherwise, we let $\beta = 1$.

The target flow rate in the next time step is

$$\tilde{q}_0(t+1) = \alpha \hat{q}_0(t+1) + (1-\alpha)\tilde{q}_0(t).$$

The advisory speed limit at $t+1$ is

$$\tilde{v}_0(t+1) = V\left(Q^{-1}(\tilde{q}_0(t+1))\right).$$

3. If $\Delta v(t) = |\tilde{v}_0(t+1) - \tilde{v}_0(t)| > \Delta v_{thr}$, then

$$\tilde{v}_0(t+1) = \begin{cases} \tilde{v}_0(t) + \Delta v_{thr} & \tilde{v}_0(t+1) > \tilde{v}_0(t) \\ \tilde{v}_0(t) - \Delta v_{thr} & \tilde{v}_0(t+1) \leq \tilde{v}_0(t) \end{cases}$$

We should let $v_{min} \leq \tilde{v}_0(t+1) \leq v_f$, i.e.,

$$\tilde{v}_0(t+1) = \max\{\min\{\tilde{v}_0(t+1), v_f\}, v_{min}\}.$$

Also we set

$$\tilde{q}_0(t+1) = Q\left(V^{-1}(\tilde{v}_0(t+1))\right).$$

4. If $t < T$, $t = t+1$ and go back to step 2; otherwise, stop iterations.

Using the settings in Step 2, the algorithm attempted to ensure that the flow rate at the bottleneck was as close as possible to the bottleneck's capacity. When the bottleneck was congested, the algorithm reduced the vehicular throughput from the SH zone. Alternatively, if the bottleneck was uncongested, the algorithm increased the maximum throughput in the SH zone to allow more vehicles to travel through the bottleneck. We also introduced a smoothing factor, α , to smooth the target flow rate in the SH zone. The value of α ranged between 0 and 1 in order to ensure smooth transitions in the flow and speed recommendations. The smoothing factors also allowed for the avoidance of frequent oscillations of vehicular throughput as well as smoothing of traffic streams.

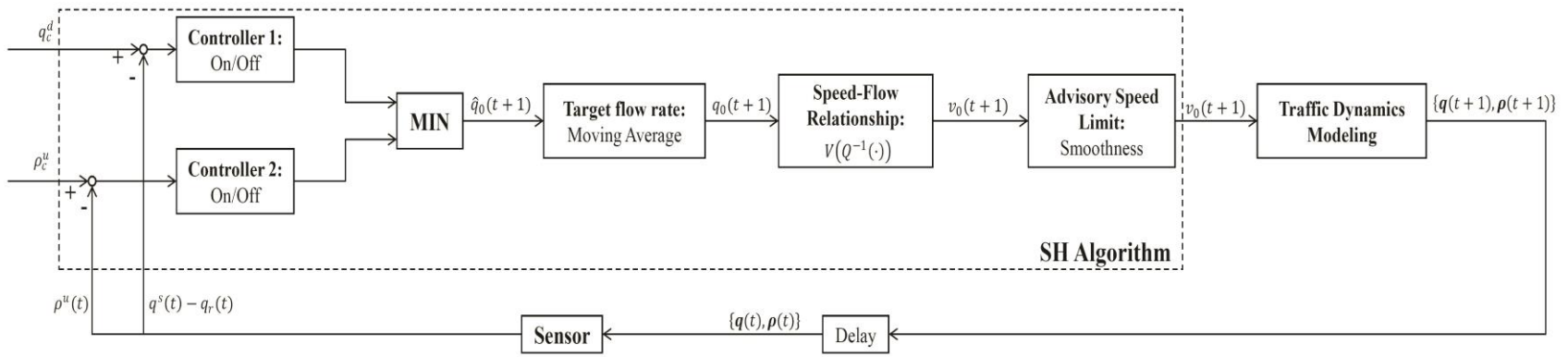


Figure 4. SH algorithm feedback control schematic.

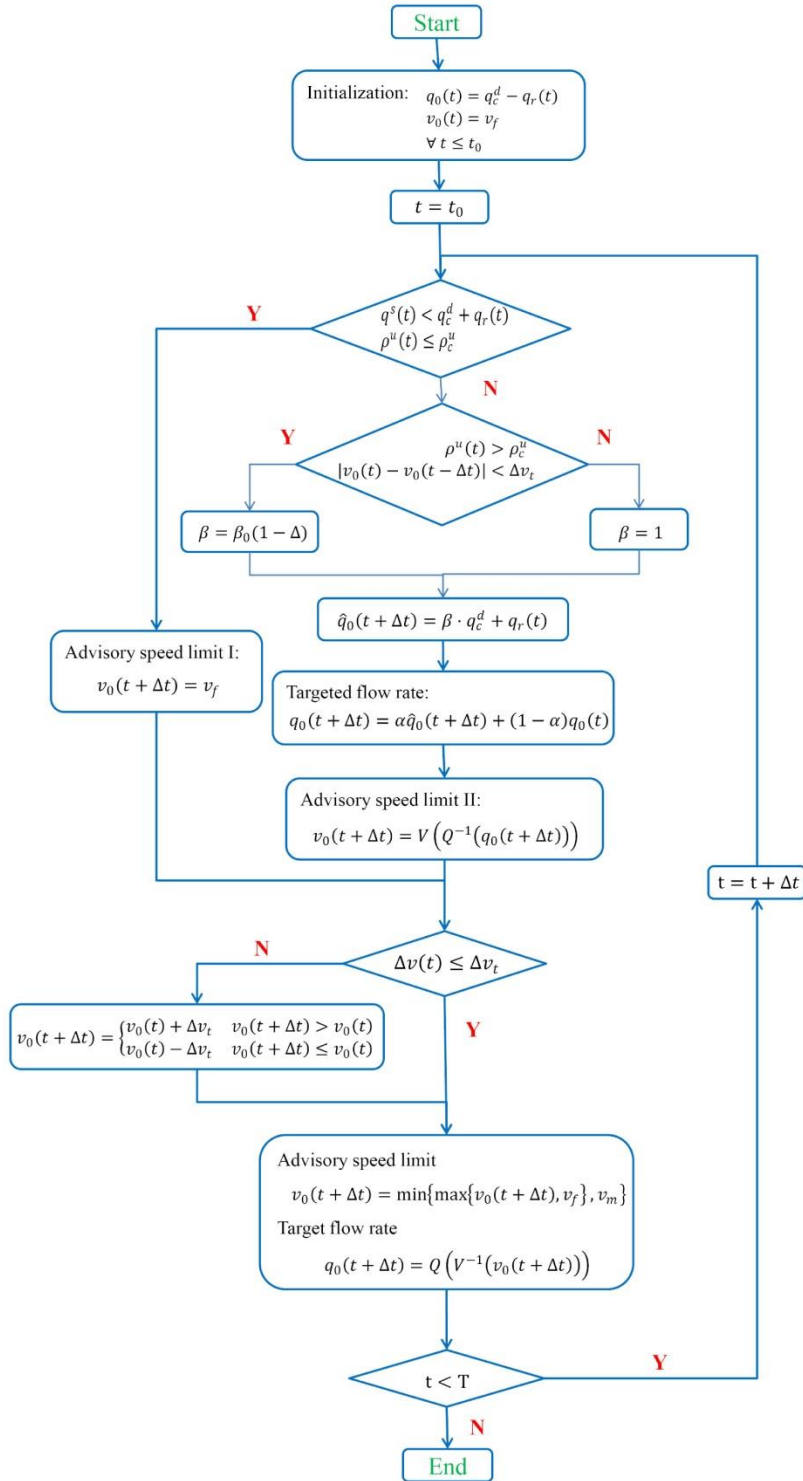


Figure 5. Flow chart of the SH algorithm.

Results and Discussion

In this project, we applied the SH algorithm that we developed to one segment of Interstate 66 in Northern Virginia to verify its benefits with INTEGRATION microscopic traffic simulation software. The results of the experiments are discussed below.

Base Case Analysis

The diagram of the roadway network segment on I-66 is illustrated in **Error! Reference source not found.** below. In the network, two freeways—Interstate 66 and Virginia State Route (SR) 267—merge together. Some basic features of the test bed are as follows:

1. The segment along I-66 is about 6-miles long, and contains several on- and off-ramps.
2. The speed limit along the mainline freeway is 105 km/hr, the road capacity is 2,000 veh/hr/lane, and the jam density is 160 veh/km/lane.
3. The number of lanes changes from four at Trailer 3 to two at Trailer 4.
4. The average travel time from the entrance of I-66 or SR-267 to the exit of I-66 is about 10 minutes.

In this experiment, we only considered traffic on the eastbound portion of the network.

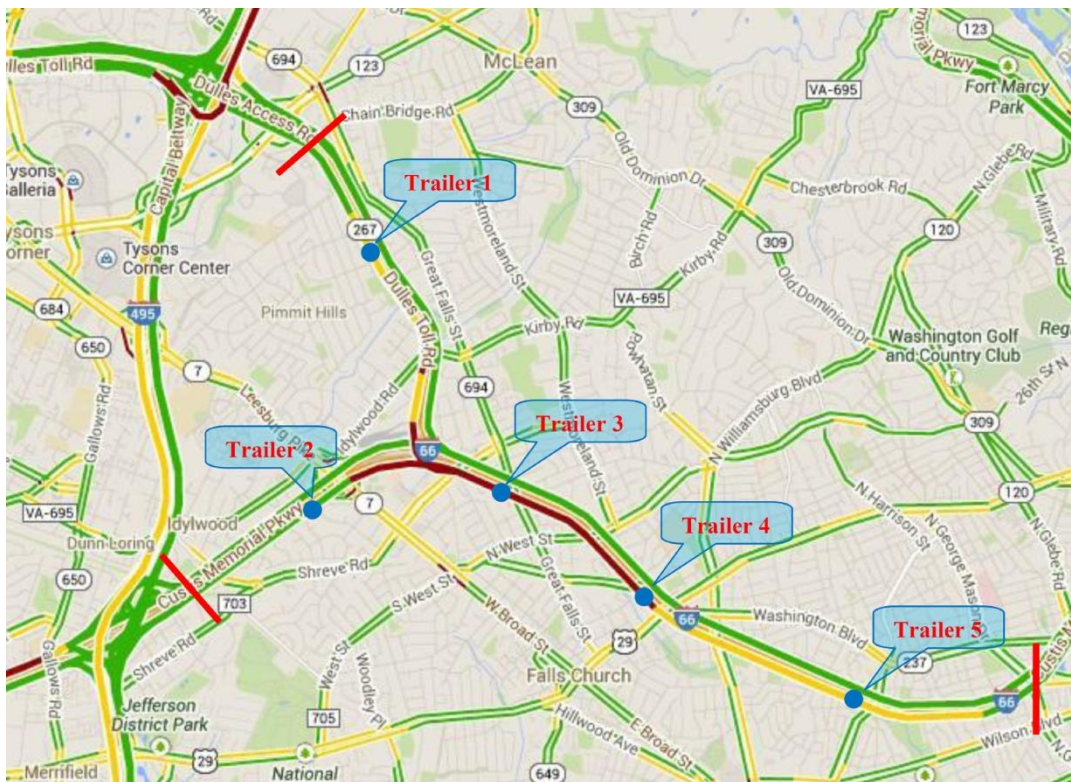


Figure 6. Diagram of I-66 network.

We obtained vehicular flow rates from the five trailers installed on the mainline freeway on March 12, 2013, and the data was applied to estimate the origin-destination tables with QueensOD [38] for the simulations. As the SH algorithm aimed to remove the capacity drop at the bottleneck, we

introduced the discharge flow rate at the bottleneck as one measurement to evaluate the SH algorithm. The delay of vehicular trips was directly related to the bottleneck capacity; with higher bottleneck capacity, traffic on the road was less congested, and the speed of vehicles was higher. This resulted in smaller average vehicular trip delays. We also investigated the benefits of the SH algorithm on emissions and fuel consumption.

In the base case analysis, the network was simulated without applying the SH algorithm to identify the location of the major bottleneck and to estimate capacity drop in the network. The SH algorithm settings were determined based on the base case analysis.

We simulated the traffic on the network for 6 hours (from 2:00 p.m.–8:00 p.m.). **Error! Reference source not found.** shows the simulated speed profiles at the five trailers. The speed first dropped at Trailer 4, propagated back to Trailer 3, and then to Trailer 2 and Trailer 1 in I-66 and SR-269, respectively. This indicated that a queue first formed at Trailer 4, where the number of lanes dropped from three to two. We also determined that Trailer 4 was the last position that the congestion was released. Hence, we set this location as the major bottleneck on the road and applied the SH algorithm to improve traffic performance at this bottleneck.

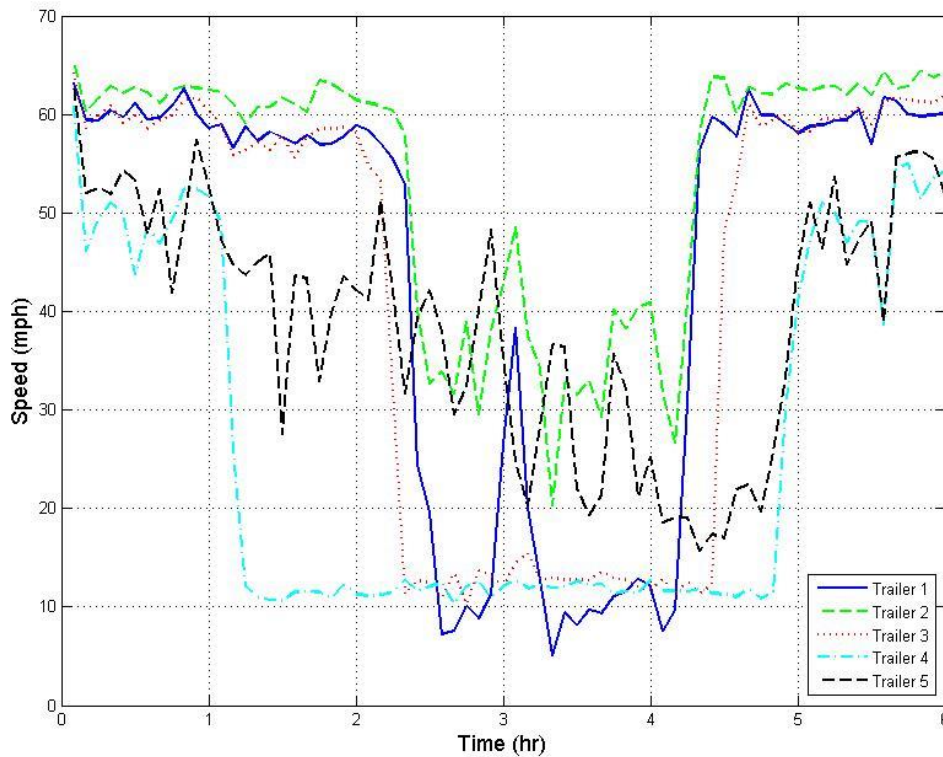


Figure 7. Speed profiles along I-66.

In the simulation, the desired flow rate through the bottleneck was set at 4,000 vph (2,000 veh/hr/lane)—the bottleneck’s capacity—during the peak-hours (3:00 p.m.–6:00 p.m.)., Due to lane changes upstream of the bottleneck, the discharge flow rate was lower than the desired value,

and a queue was generated at the upstream of the bottleneck, causing capacity drop. **Error! Reference source not found.** shows that the discharge flow rate at the downstream of the bottleneck was only 1,500 veh/hr/lane, which means the capacity drop was about 25%, representing a critical limitation of the network performance. In the following section, we will examine the application of the SH algorithm to improve the network's overall traffic conditions.

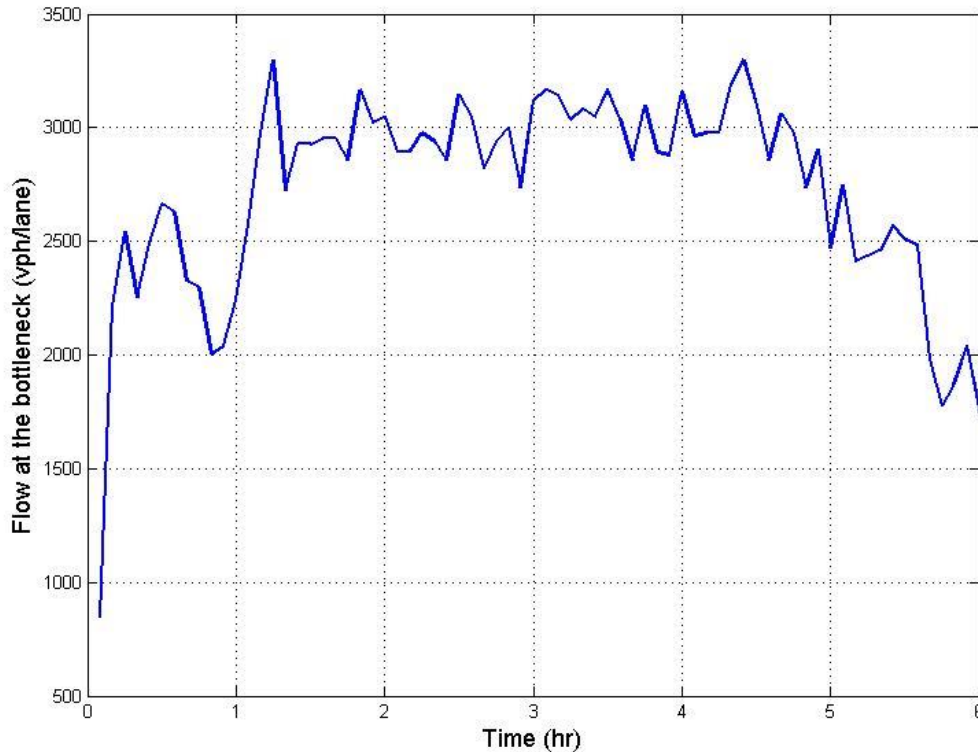


Figure 8. Flow rate at the bottleneck.

Case study I: SH Algorithm and Three V2I-Equipped Vehicles

In the first case study, we applied the SH algorithm to the network for the bottleneck identified in **Error! Reference source not found.**, and investigated the influence of the algorithm on the driving behaviors of V2I-equipped vehicles. In the experiment, three equipped vehicles were assigned to enter the network from the entrance of I-66 during peak hours. The segment on I-66 between Trailer 3 and North West Street was defined as the SH zone. There were two off-ramps between the SH zone and the bottleneck. Three detectors were installed at the end of the SH zone, the upstream of the bottleneck, and the off-ramps to collect traffic information.

Table 1. Settings of the SH Algorithm

Parameters	Values
$q_{d,c}$	2000 veh/h/lane
$\rho_{u,c}$	22.2 veh/km/lane
α	0.5
β_0	0.9
γ	0.5
Δv_t	16 km/h
v_m	40 km/h
Δt	30 seconds
T	6 h
t_0	0.5 h

Error! Reference source not found. shows the SH algorithm's settings. The advisory speed limit sent to the equipped vehicles in the SH zone was updated at every 30 seconds, and the maximum speed limit change was 16 km/hr to avoid sharp accelerations or abrupt decelerations. The minimum speed limit was set at 40 km/hr to avoid extremely slow traffic. Additionally, no equipped vehicles in the SH zone were allowed to exceed the advisory speed limit.

Error! Reference source not found. compares the speed profiles of one equipped vehicle before and after applying the SH algorithm. Clearly, the speed of the equipped vehicle was gradually reduced in the SH zone, and the vehicle was allowed to travel faster at the downstream of the bottleneck. This figure illustrates that the SH algorithm was able to adjust the equipped vehicles' speed based on the road conditions. However, with the SH algorithm in use, the equipped vehicles had to travel more slowly to restrict through traffic, resulting in other vehicles attempting passing maneuvers. As a result, through traffic congestion was still larger than the desired value, and the upstream of the bottleneck was still congested. As long as other vehicles were passing slowed equipped vehicles, capacity drop could not be prevented, leading us to conclude that three equipped vehicles alone cannot improve the overall network performance. **Error! Reference source not found.** compares the delay of vehicular trips, discharge flow rates at the bottleneck, emissions, and fuel consumption before and after applying the SH algorithm. The differences of delay and flow rate at the bottleneck were very small (<0.4%), and the differences in emission and fuel consumption were less than 0.7%. The results show that applying the SH algorithm with only three equipped vehicles is meaningless to in terms of road performance.

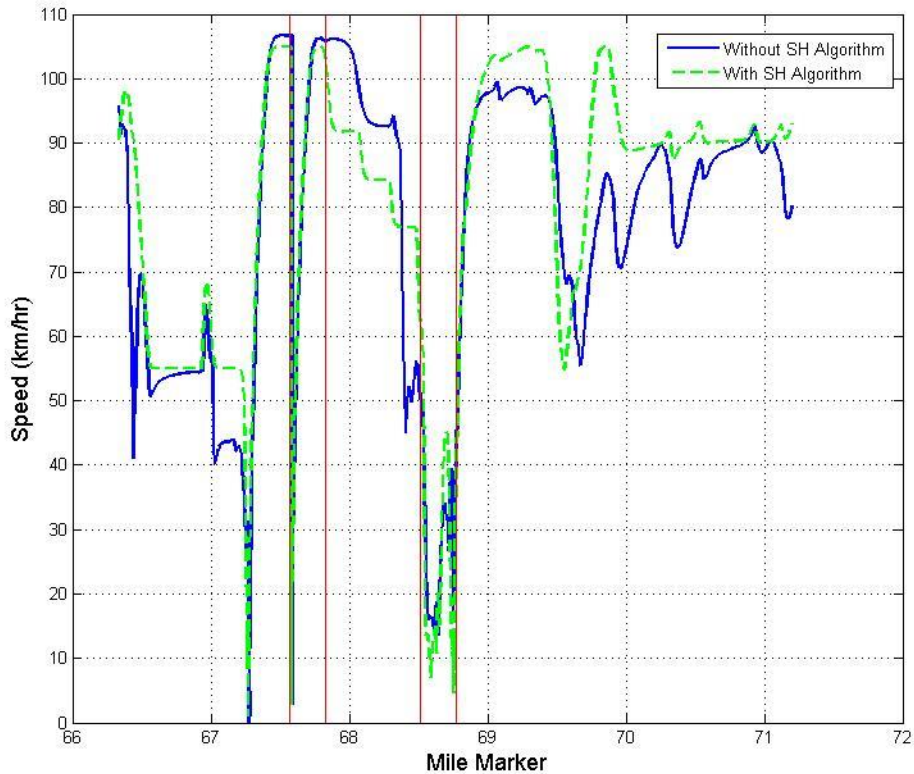


Figure 9. Comparison of speed profiles on I-66 with three vehicles.

Table 2. Simulation Results with Three Equipped Vehicles

Parameters	Fuel (l/km)	HC (g/km)	CO (g/km)	NOx (g/km)	CO ₂ (g/km)	Delay (s/km)	Flow @ bottleneck (veh/h/lane)
Base	0.120	0.568	14.50	0.364	257.2	24.92	1502
SH algorithm	0.120	0.565	14.41	0.363	257.4	25.02	1503
Diff (%)	0.00	-0.56	-0.62	-0.10	0.08	0.40	0.07

Case Study II: SH Algorithm and 100% V2I-Equipped Vehicles

In the second case study, we investigated the benefits of the SH algorithm with a 100% equipped vehicle market penetration rate (i.e., all vehicles in the simulation received advisory speed limits from the SH algorithm). The SH algorithm settings in **Error! Reference source not found.** were also applied in this experiment.

Here, we compared the total delay of vehicular trips, discharge flow rate at the bottleneck, emissions, and fuel consumption before and after applying the SH algorithm. The results in **Error! Reference source not found.** show that the discharge flow rate at the bottleneck was improved by about 1.56%, while vehicular trip delays were reduced more than 22%. Also, there were more than 3% savings on CO₂ and fuel consumption as well as on other vehicle emissions. The table clearly verifies the benefits of the SH algorithm on network performance.

Table 3. Simulation Results with 100% Equipped Vehicles

Parameters	Fuel (l/km)	HC (g/km)	CO (g/km)	NOx (g/km)	CO2 (g/km)	Delay (s/km)	Flow @ bottleneck (vph/lane)
Base	0.120	0.568	14.50	0.364	257.2	24.92	1502
SH algorithm	0.1115	0.520	13.04	0.357	248.9	19.38	1521
Diff (%)	-3.47	-8.53	-10.07	-1.93	-3.20	-22.24	1.56

We also compared the peak-hour average speed along I-66 before and after applying the SH algorithm. The results are shown in **Error! Reference source not found.**. As the exiting flow rate of the SH zone was controlled with the SH algorithm, the upstream of the bottleneck was less congested and the speed was higher, indicating a large improvement in the bottleneck condition. This also explains the huge savings on the total delay of vehicular trips.

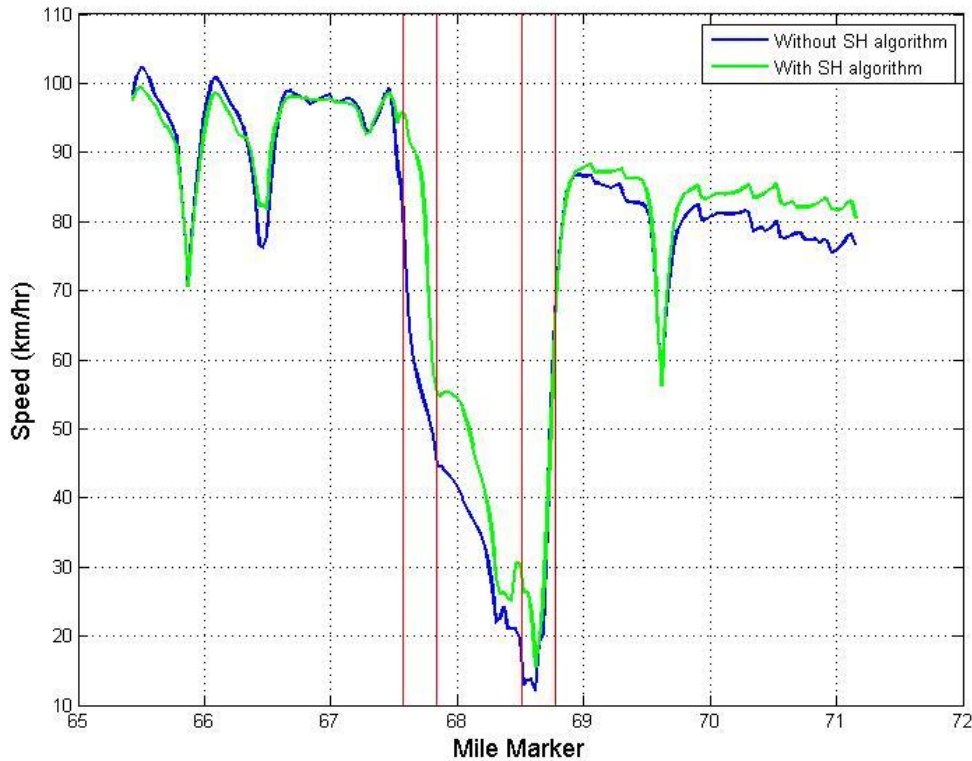


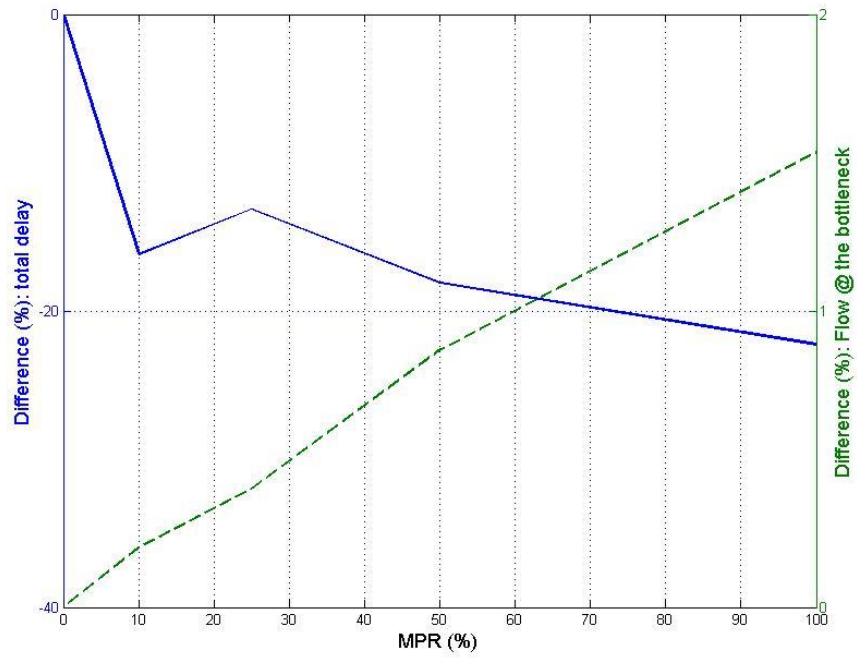
Figure 10. Comparison of speed profiles along I-66 with 100% equipped vehicles.

Case Study III: Different Market Penetration Rates

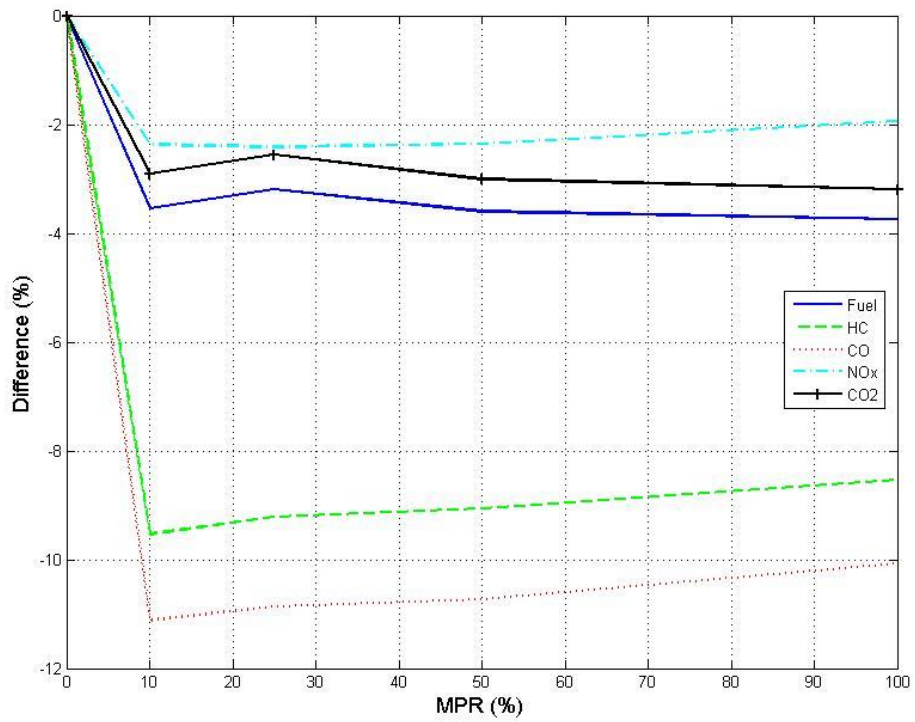
In the third case study, we investigated the influence of equipped vehicle market penetration rates on the SH algorithm. The I-66 network was also applied, and we used the same settings given in **Error! Reference source not found.** to implement the SH algorithm. As with the first SH algorithm case study, equipped vehicles were controlled by the advisory speed limit, which was

usually slower than their prevailing traffic. In that sense, when the MPR of equipped vehicles was smaller, more vehicles without V2I communications were willing to pass the slower equipped vehicles. This resulted in more lane changes in the SH zone, and the exiting flow rate of the SH zone was larger than the desired value determined by the SH algorithm. Hence, the algorithm worked less effectively. With higher MPRs, less vehicle passing was likely to occur. Therefore, higher MPRs can be conclusively found to have improved the benefits of the SH algorithm.

In this experiment, we introduced various MPRs—0, 0.1, 0.25, 0.5, and 1—to analyze the impact of MPRs on SH algorithm benefits. The simulation results, provided in **Error! Reference source not found.a** and **Error! Reference source not found.b**, show that with higher MPRs, the discharge flow rate at the bottleneck was larger, the total delay of vehicular trips was smaller, and that emissions and fuel consumption savings were greater. Once $\text{MPR} \geq 10\%$ —approximately 120 veh/hr/lane in this example—the benefits of the SH algorithm on reducing emissions and fuel consumption were not significantly different, indicating that with the proposed SH algorithm, an MPR of 10% equipped vehicles is enough to reduce emissions and fuel consumption. In the simulation, we observed that a 10% MPR of equipped vehicles comprised a high enough rate of traffic that non-equipped vehicles rarely passed the equipped vehicles ahead. Essentially, the behaviors of the non-equipped vehicles were controlled by the equipped vehicles, and the SH algorithm could be considered effective at 10% MPR. With even higher MPRs, as more vehicles comply with the advisory speed limits to maximize the discharge flow rate of the bottleneck, the rate of the bottleneck can be improved even more, and vehicles on the network can travel faster with smaller delay.



(a)



(b)

Figure 11. Impact of MPRs on the SH algorithm: (a) delay and flow rate at the bottleneck, (b) emissions and fuel consumption.

Conclusions

This project developed a bi-level feedback control speed harmonization algorithm to prevent capacity drop at bottlenecks and to mitigate road congestion. The algorithm computed and transmitted advisory speed limits to individual vehicles through a V2I communication system. The SH algorithm's advisory speed limits were determined by individual vehicle speeds, the density at the bottleneck, and the exiting flow rate of the SH zone. In addition, the limits were smoothed to avoid abrupt deceleration or aggressive accelerations, which may have posed safety hazards. One 6-mile segment of I-66 in Northern Virginia was simulated to examine the effectiveness of the algorithm. When the algorithm was applied, the speed of the equipped vehicles decreased gradually to restrict the arrival rates at the downstream bottleneck and mitigate traffic congestion.

This project demonstrated that applying the SH algorithm to only a few vehicles rarely affected the performance of the whole network, as the equipped vehicles traveled slower than the prevailing traffic and were overtaken by other vehicles, reducing the effectiveness of the algorithm. But, with higher market penetration rates of equipped vehicles, the discharge flow rate of the bottleneck was larger, and both the traffic stream delay and vehicle emissions and fuel consumption levels were reduced. The simulation results showed that a 10% MPR was sufficient for the SH algorithm to reduce emissions and fuel consumption levels; however, the discharge flow rate and the delay did not reach their optimal values at 10% MPR. With a 100% MPR, the discharge flow rate increased by more than 1.5%, the delay decreased by more than 22%, and CO₂ and fuel consumption levels were reduced by up to 3.5% for the entire network.

References

1. Parry, M. L., *Climate Change 2007: impacts, adaptation and vulnerability*. Cambridge University Press, 2007, vol. 4.
2. Faiz, A., “Automotive emissions in developing countries-relative implications for global warming, acidification and urban air quality,” *Transportation Research Part A*, vol. 27, no. 3, pp. 167–186, 1993.
3. Schrank, D., B. Eisele, and T. Lomax, “2012 urban mobility report,” Texas A&M Transportation Institute, Texas, USA, Tech. Rep., 2012.
4. Edie, L. C., “Car-following and steady-state theory for noncongested traffic,” *Operations Research*, vol. 9, no. 1, pp. 66–76, 1961.
5. Banks, J. H., “The two-capacity phenomenon: some theoretical issues,” *Transportation Research Record*, vol. 1320, no. 1, pp. 234–241, 1991.
6. Hall, F. L., and K. Agyemang-Duah, “Freeway capacity drop and the definition of capacity,” *Transportation Research Record*, vol. 1320, no. 1, pp. 91–98, 1991.
7. Cassidy, M. J., “Bivariate relations in nearly stationary highway traffic,” *Transportation Research Part B*, vol. 32, no. 1, pp. 49–59, 1998.
8. Cassidy, M. J., and R. L. Bertini, “Some traffic features at freeway bottlenecks,” *Transportation Research Part B*, vol. 33, no. 1, pp. 25–42, 1999.
9. Persaud, B., S. Yagar, and R. Brownlee, “Exploration of the breakdown phenomenon in freeway traffic,” *Transportation Research Record*, vol. 1634, no. 1, pp. 64–69, 1998.
10. Rakha, H., and M. Van Aerde, “Integration c release 2.50 for windows: User’s guide—volume i: Fundamental model features,” M. Van Aerde & Assoc., Ltd., Blacksburg, VA USA, Tech. Rep., 2013.
11. Rakha, H., and M. Van Aerde, “Integration c release 2.50 for windows: User’s guide—volume ii: Advanced model features,” M. Van Aerde & Assoc., Ltd., Blacksburg, VA USA, Tech. Rep., 2013.
12. Chamberlayne, E., H. Rakha, and D. Bish, “Modeling the capacity drop phenomenon at freeway bottlenecks using the integration software,” *Transportation Letters*, vol. 4, no. 4, pp. 227–242, 2012.
13. Papageorgiou, M., H. Hadj-Salem, and J.-M. Blosseville, “Alinea: A local feedback control law for on-ramp metering,” *Transportation Research Record*, vol. 1320, no. 1, pp. 58–64, 1991.
14. Papageorgiou, M., H. Hadj-Salem, and F. Middelham, “Alinea local ramp metering: Summary of field results,” *Transportation Research Record*, vol. 1603, no. 1, pp. 90–98, 1997.
15. Haj-Salem, H., and M. Papageorgiou, “Ramp metering impact on urban corridor traffic: Field results,” *Transportation Research Part A*, vol. 29, no. 4, pp. 303–319, 1995.
16. Munoz, J. C., and C. F. Daganzo, “The bottleneck mechanism of a freeway diverge,” *Transportation Research Part A*, vol. 36, no. 6, pp. 483–505, 2002.

17. Cassidy, M. J., "Freeway on-ramp metering, delay savings, and diverge bottleneck," *Transportation Research Record*, vol. 1856, no. 1, pp. 1–5, 2003.
18. Cassidy, M. J., and J. Rudjanakanoknad, "Increasing the capacity of an isolated merge by metering its on-ramp," *Transportation Research Part B*, vol. 39, no. 10, pp. 896–913, 2005.
19. Chung, K., J. Rudjanakanoknad, and M. J. Cassidy, "Relation between traffic density and capacity drop at three freeway bottlenecks," *Transportation Research Part B*, vol. 41, no. 1, pp. 82–95, 2007.
20. Lentzakis, A. F., A. D. Spiliopoulou, I. Papamichail, M. Papageorgiou, and Y. Wang, "Real-time work zone management for throughput maximization," in *Transportation Research Board 87th Annual Meeting, Washington, DC*, 2008.
21. Tympakianaki, A., A. Spiliopoulou, A. Kouvelas, I. Papamichail, M. Papageorgiou, and Y. Wang, "Real-time merging traffic control for throughput maximization at motorway work zones," *Transportation Research Part C*, vol. 44, pp. 242–252, 2014.
22. Papageorgiou, M., I. Papamichail, A. Spiliopoulou, and A. Lentzakis, "Real-time merging traffic control with applications to toll plaza and work zone management," *Transportation Research Part C*, vol. 16, no. 5, pp. 535–553, 2008.
23. Spiliopoulou, A. D., I. Papamichail, and M. Papageorgiou, "Toll plaza merging traffic control for throughput maximization," *Journal of Transportation Engineering*, vol. 136, no. 1, pp. 67–76, 2009.
24. Hegyi, A., B. De Schutter, and J. Hellendoorn, "Optimal coordination of variable speed limits to suppress shock waves," *IEEE Transactions on Intelligent Transportation Systems*, vol. 6, no. 1, pp. 102–112, 2005.
25. Hegyi, B. De Schutter, and H. Hellendoorn, "Model predictive control for optimal coordination of ramp metering and variable speed limits," *Transportation Research Part C*, vol. 13, no. 3, pp. 185–209, 2005.
26. Carlson, R. C., I. Papamichail, M. Papageorgiou, and A. Messmer, "Optimal mainstream traffic flow control of large-scale motorway networks," *Transportation Research Part C*, vol. 18, no. 2, pp. 193–212, 2010.
27. Carlson, R. C., I. Papamichail, and M. Papageorgiou, "Local feedback based mainstream traffic flow control on motorways using variable speed limits," *IEEE Transactions on Intelligent Transportation Systems*, vol. 12, no. 4, pp. 1261–1276, 2011.
28. Carlson, R. C., I. Papamichail, and M. Papageorgiou, "Comparison of local feedback controllers for the mainstream traffic flow on freeways using variable speed limits," *Journal of Intelligent Transportation Systems*, vol. 17, no. 4, pp. 268–281, 2013.
29. Carlson, R. C., I. Papamichail, and M. Papageorgiou, "Integrated feedback ramp metering and mainstream traffic flow control on motorways using variable speed limits," *Transportation research part C*, vol. 46, pp. 209–221, 2014.

30. Rauh Muller, E., R. Castelan Carlson, W. Kraus, and M. Papageorgiou, "Microsimulation analysis of practical aspects of traffic control with variable speed limits," *IEEE Transactions on Intelligent Transportation Systems*, vol. 16, no. 1, pp. 512–523, 2015.
31. Jin, H.-Y., and W.-L. Jin, "Control of a lane-drop bottleneck through variable speed limits," *arXiv preprint arXiv:1310.2658*, 2013.
32. Chen, D., S. Ahn, and A. Hegyi, "Variable speed limit control for steady and oscillatory queues at fixed freeway bottlenecks," *Transportation Research Part B*, vol. 70, pp. 340–358, 2014.
33. Chen, D., and S. Ahn, "Variable speed limit control for severe nonrecurrent freeway bottlenecks," *Transportation Research Part C*, vol. 51, pp. 210–230, 2015.
34. Laval, J. A., and C. F. Daganzo, "Lane-changing in traffic streams," *Transportation Research Part B*, vol. 40, no. 3, pp. 251–264, 2006.
35. Yang, H., and H. Rakha, "Developemnt of a speed harmonization algorithm: Methodology and preliminary testing," 2015, submitted to *Transportation Research Part B*.
36. Rakha, H., K. Ahn, and A. Trani, "Development of vt-micro model for estimating hot stabilized light duty vehicle and truck emissions," *Transportation Research Part D*, vol. 9, no. 1, pp. 49–74, 2004.
37. Rakha, H., "Queensod rel. 2.10-user guide: Estimating origin-destination traffic demands from link flow counts," 2002.